Motion in a Bose condensate: IX. Crow instability of antiparallel vortex pairs

2001 J. Phys. A: Math. Gen. 34 10057

(http://iopscience.iop.org/0305-4470/34/47/311)

INSTITUTE OF PHYSICS PUBLISHING JOURNAL OF PHYSICS A: MATHEMATICAL AND GENERAL

J. Phys. A: Math. Gen. **34** (2001) 10057–10066 PII: S0305-4470(01)26316-1

Motion in a Bose condensate: IX. Crow instability of antiparallel vortex pairs

Natalia G Berloff and Paul H Roberts

Department of Mathematics, University of California, Los Angeles, CA 90095-1555, USA

E-mail: nberloff@math.ucla.edu and roberts@math.ucla.edu

Received 27 June 2001
Published 16 November 2001
Online at stacks.iop.org/JPhysA/34/10057

Abstract

The Gross–Pitaevskii (GP) equation admits a two-dimensional solitary wave solution representing two mutually self-propelled, antiparallel straight line vortices. The complete sequence of such solitary wave solutions has been computed by Jones and Roberts (Jones C A and Roberts P H 1982 *J. Phys. A: Math. Gen.* **15** 2599). These solutions are unstable with respect to three-dimensional perturbations (the Crow instability). The most unstable mode has a wavelength along the direction of the vortices of the same order as their separation. The growth rate associated with this mode is evaluated here and it is found to increase very rapidly with decreasing separation. It is shown, through numerical integrations of the GP equation that, as the perturbations grow to finite amplitude, the lines reconnect to produce a sequence of almost circular vortex rings.

PACS numbers: 03.75.Fi, 47.37.+q

1. Introduction

The experimental realization of the Bose–Einstein condensation in trapped alkali-metal gases at ultralow temperatures has stimulated a tremendous interest in the production of vortices and vortex arrays and theoretical investigations of their structure, energy, dynamics and stability (for a comprehensive review see [4]). The main theoretical tool for these studies is the Gross–Pitaevskii (GP) model which represents the so-called mean-field limit of quantum field theories. The same equation has been the subject of extensive studies also in the framework of superfluid helium at very low temperature. In this case the GP model is assumed to be linked to the condensate fraction of the superfluid, although the resulting theory is at best a qualitative description of superfluid helium.

This is the ninth in a series of papers devoted to modelling flows in a Bose condensate. Reference will be made to the fourth and fifth papers in the sequence [6, 7]. In contrast to

the atomic condensates, where the material lies in a trap and is significantly non-uniform, this sequence of papers, including the present paper, considers only uniform backgrounds.

Superfluid turbulence is the focus of many experimental and theoretical studies [3]. This manifests itself as a tangle of quantized vortex lines. The dynamics of the tangle depends crucially on the interactions of the vortex filaments. These have been studied by using the classical model of vortices in an incompressible Euler fluid. This omits, however, two mechanisms that are very relevant to the superfluid tangle.

First, as Vinen [21] argues, emission of sound by a vortex tangle is very significant in superfluid turbulence. This process is completely removed by the main assumption of classical vortex theory: $\nabla \cdot \boldsymbol{v} = 0$, where $\boldsymbol{v}$ is the superfluid velocity. The dynamics of vortex filaments in a compressible fluid is not understood as well as that for the incompressible case. The scattering of sound by compressible Euler fluids has, however, been the subject of several recent investigations (see e.g. [5]).

Second, the processes of severance and coalescence of vortex lines are centrally important for the study of superfluid turbulence, but these are expressly forbidden by the Kelvin–Helmholtz theorem, according to which vortex lines are frozen to an Euler fluid and cannot change their topology. In an Euler fluid, the processes have been successfully simulated numerically by restoring viscosity. This step is disallowed in a superfluid and the only way to defeat the theorem is through *ad hoc* procedures. For example, it was supposed by Schwarz [20] that, whenever one vortex filament comes within a distance Δ of another filament, reconnection will always occur and that otherwise reconnection will not happen. A precise way of determining Δ is not known, but its value can greatly affect the reconnection rate in a vortex tangle. Moreover, the angle at which the vortex filaments approach one another is undoubtedly an important factor in determining whether they reconnect or not; a clear set of reconnection rules is lacking.

The advantage of GP theory in comparison with the classical approach is that it gives superfluid vortex lines their own unique core structure. At the same time, it provides a mechanism for the severance and coalescence of vortex lines, and includes sound propagation, so that the acoustic emission from a vortex tangle can be evaluated. Koplik and Levine [8, 9] used numerical simulations of the GP model to study the reconnection of, and the interaction between, straight-line vortices and vortex rings. In particular, they witnessed the annihilation of vortex rings of similar radii. Recently Leadbeater *et al* [12] elucidated the loss of energy to sound emission during vortex ring collisions. Their calculations suggested that the sound emitted during reconnections is a significant decay mechanism for superfluid turbulence.

In this paper, we first study the linear stability of a vortex pair. This is a two-dimensional (2D) structure that can, in GP theory, be represented by a wavefunction $\psi_0(x, y, t)$ which is independent of the coordinate z and has two zeros at $y = \pm\frac{1}{2}h$, representing vortices separated by a distance h. The phase of ψ_0 increases by 2π round one zero and decreases by 2π round the other corresponding, in the hydrodynamic interpretation of ψ_0, to a pair of antiparallel vortices (sometimes called 'point vortices') that move uniformly with speed U in the x-direction as a solitary wave, i.e., $\psi_0 = \psi_0(x - Ut, y)$, where U is obtained by solving the GP equation in 2D:

$$2\mathrm{i}U\frac{\partial\psi_0}{\partial x} = \frac{\partial^2\psi_0}{\partial x^2} + \frac{\partial^2\psi_0}{\partial y^2} + \left(1 - |\psi_0|^2\right)\psi_0. \tag{1}$$

(Here, and frequently in what follows, we use dimensionless variables such that the unit length corresponds to the healing length a, the speed of sound is $c = 1/\sqrt{2}$ and the density at infinity is $\rho_\infty = 1$. Later we shall write $\psi_0 = u_0 + \mathrm{i}v_0$, where u_0 and v_0 are real.) Solutions of this form were first reported by Jones and Roberts [6] who determined the entire sequence of such

solutions and their associated energy per unit length $\mathcal{E}$ and momentum per unit length $\mathcal{P}$, both of which decrease to zero as $h \to 0$:

$$\mathcal{E} = \frac{1}{2}\int |\nabla\psi_0|^2\,\mathrm{d}V + \frac{1}{4}\int \left(1-|\psi_0|^2\right)^2\,\mathrm{d}V \tag{2}$$

$$\mathcal{P} = \frac{1}{2\mathrm{i}}\int [(\psi_0^*-1)\nabla\psi_0 - (\psi_0-1)\nabla\psi_0^*]\,\mathrm{d}V. \tag{3}$$

Multiplying (1) by $x\partial\psi_0^*/\partial x$ and integrating by parts, Jones *et al* [7] showed that

$$\mathcal{E} = \frac{1}{2}\int \left|\frac{\partial\psi_0}{\partial x}\right|^2 \mathrm{d}V. \tag{4}$$

They located a critical value $h_c \approx 1.7$ of h, at which the sequence lost or gained vorticity. For $h < h_c$, the sequence has no vorticity, although solitary disturbances exist as finite amplitude sound waves in which the two minima of $|\psi_0|$ are no longer zero. As $h \to 0$, U approaches the speed of sound c and the acoustic solutions merge with the phonon branch of the dispersion curve.

Jones and Roberts did not examine the stability of their 2D solitary waves. It is known that the vortex pair in an incompressible Euler fluid is prone to the so-called 'Crow instability' [2]. Kuznetsov and Rasmussen [10] proved that in the long-wavelength limit, where k is small compared with h, both the vortex pair and solitary acoustic solutions are unstable, but they determined neither the boundaries of instability nor the wavelength at which the growth rate is maximal. In this paper we first solve the linear stability problem for all h with the particular aim of finding the growth rate of the Crow instabilities as a function of the separation h. We study the subsequent evolution of the instabilities to finite amplitude by integrating the GP equations in 3D. This parallels the corresponding analysis by Moore [13] for a classical fluid, but differs in that healing becomes important as the instability brings one vortex core close to the other. Unlike the classical case, reconnection can, and does, occur so that the final result is a sequence of almost circular vortex rings.

2. Linear stability of the vortex pair

We return to the GP equation in the reference frame moving with the vortex pair

$$-2\mathrm{i}\frac{\partial\psi}{\partial t} + 2\mathrm{i}U\frac{\partial\psi}{\partial x} = \nabla^2\psi + (1-|\psi|^2)\psi. \tag{5}$$

We seek solutions of (5) in the form $\psi(x,y,z,t) = \psi_0(x,y) + \hat{\psi}(x,y,z,t)$ where $\hat{\psi}$ is infinitesimal. The resulting linearized GP equation determines the stability of the vortex pair. We separate $\hat{\psi}$ into real and imaginary parts, $\hat{u}$ and $\hat{v}$, and focus on separable solutions of the form

$$\hat{u} = u(x,y)\exp[\sigma t - \mathrm{i}kz] + u^*(x,y)\exp[\sigma t + \mathrm{i}kz] \tag{6}$$

and similarly for $\hat{v}$, where $*$ stands for complex conjugation; the functions u and v are governed by

$$\nabla_{xy}^2 u + 2U\frac{\partial v}{\partial x} + \left(1-3u_0^2-v_0^2-k^2\right)u - 2u_0v_0v = 2\sigma v \tag{7}$$

$$\nabla_{xy}^2 v - 2U\frac{\partial u}{\partial x} + \left(1-u_0^2-3v_0^2-k^2\right)v - 2u_0v_0u = -2\sigma u \tag{8}$$

and, since the perturbation must vanish at great distances from the vortex pair, we have

$$u \to 0 \qquad v \to 0 \qquad \text{for} \quad s \equiv \sqrt{x^2+y^2} \to \infty. \tag{9}$$

The linear stability problem posed by (7)–(9) has features in common with the corresponding classical stability problem analysed by Crow [2]. In particular, it follows from (7)–(9) that σ^2 is real. This may be demonstrated by introducing adjoint variables $\bar{u}$ and $\bar{v}$ that obey (9) and share the same eigenvalue spectrum. We multiply (7) by $\bar{u}$, (8) by $\bar{v}$, add corresponding sides, integrate over the interior of the cylinder $s = S$, apply the divergence theorem, discarding the resulting surface integrals for $S \to \infty$ by an appeal to (9). We then find that $\bar{u}$ and $\bar{v}$ must obey (7)–(9), but with σ replaced by $-\sigma$. In short, if σ is an eigenvalue of (7)–(9), so is $-\sigma$. Since all the coefficients in (7) and (8) are real, σ and σ^* are both eigenvalues. Thus in all cases σ^2 is real.

The eigenvalues of (7)–(9) belong to two distinct types of instability, termed the symmetric and the antisymmetric modes:

$$\begin{aligned} &\text{symmetric:} \qquad u(-x, y) = -u(x, y) \qquad v(-x, y) = v(x, y) \\ &\text{antisymmetric:} \quad u(-x, y) = u(x, y) \qquad v(-x, y) = -v(x, y). \end{aligned}$$

Kuznetsov and Rasmussen [10] demonstrated that all long-wavelength antisymmetric modes are stable and all long-wavelength symmetric modes are unstable. In fact, they showed that the dispersion relation for the antisymmetric perturbation is

$$\sigma^2 = (kU)^2\left(1 - \frac{\mathcal{E}}{\mathcal{P}U}\right) < 0 \qquad k \to 0 \tag{10}$$

and the growth rate of symmetric perturbation is given by

$$\sigma^2 = -\frac{\mathcal{E}}{\partial\mathcal{P}/\partial U}k^2 > 0 \qquad k \to 0 \tag{11}$$

where $\mathcal{E}$ and $\mathcal{P}$ are the energy and momentum per unit length of the vortex pair; see (2) and (3). These have been evaluated by Jones and Roberts [6] and Jones *et al* [7] for the entire vortex sequence, from the KP1-soliton for $\mathcal{P} \to 0$ to a widely separated pair of vortices for $\mathcal{P} \to \infty$. In the latter case it was found that, in dimensional units,

$$\mathcal{E} \sim \frac{\rho_\infty \kappa^2}{2\pi}\left[\ln\frac{h}{a} + \alpha\right] \tag{12}$$

$$\mathcal{P} \sim \rho\kappa h \qquad U \sim \frac{\kappa}{2\pi h} \tag{13}$$

where a is the healing length and α is the vortex core parameter determined numerically by Pitaevskii as $\alpha \approx 0.38$ [14]. To compare (11) with the result obtained by Crow [2] we rewrite (12) using the cut-off method [19]. According to this method we estimate the vortex cut-off parameter δ by comparing the velocity of a ring of radius R given by the cut-off formula

$$U = \frac{\kappa}{16\pi R}\int_{a\delta/R}^{2\pi - a\delta/R} \frac{1}{\sin\frac{1}{2}\theta}\,\mathrm{d}\theta = \frac{\kappa}{4\pi R}\ln\frac{4R}{a\delta} \tag{14}$$

with the analytical result [18]

$$U = \frac{\kappa}{4\pi R}\left(\ln\frac{8R}{a} - 1 + \alpha\right). \tag{15}$$

This comparison gives us

$$\ln 2\delta = 1 - \alpha. \tag{16}$$

Using (16) as a definition of the cut-off parameter for the GP model we can write (12) as

$$\mathcal{E} \sim \frac{\rho_\infty \kappa^2}{2\pi}\left[\ln\frac{h}{2a\delta} + 1\right] \tag{17}$$

which together with (13) and (11) implies that, for symmetric modes,

$$\sigma^2 \sim \left(\frac{\kappa}{2\pi h}\right)^2 k^2\left[\ln\frac{h}{2a\delta}+1\right] \qquad k\to 0. \tag{18}$$

This establishes that they are unstable for all sufficiently large wavelengths.

It is possible here to compare (18) with the classical theory of Crow [2], in which δ is the cut-off employed when vorticity is assumed to be confined to filaments. Crow assumed the uniform core vortex model, but his derivation is easily adapted to a vortex pair with other core structures. He found that, provided $ka \ll 1$, where a is the core radius,

$$\sigma^2 = \left(\frac{\kappa}{2\pi h^2}\right)^2\left[1+khK_1(kh)+\tfrac{1}{2}(kh)^2\omega(ak\delta)\right] \times\left[1-khK_1(kh)-(kh)^2K_0(kh)-\tfrac{1}{2}(kh)^2\omega(ak\delta)\right] \tag{19}$$

where K_0 and K_1 are modified Bessel functions, and

$$\omega(ak\delta) = -2\int_{ak\delta}^{\infty}(\cos u + u\sin u - 1)\frac{\mathrm{d}u}{u^3} \sim \ln(ak\delta)+\gamma-\tfrac{1}{2}+\mathcal{O}(ak\delta)^2. \tag{20}$$

Here $\gamma \approx 0.577216\cdots$ is Euler's constant. When we approximate (19) for $kh \ll 1$, we obtain (18).

Now we address the question of whether the expression (11) has a more general meaning and is valid for the classical core models, so that we can adopt (18) as the general expression for the growth rate of large wavelength perturbations. For the uniform core model we relate (14) to the analytical expression for the velocity of a vortex ring of radius $R \gg a$:

$$U = \frac{\kappa}{4\pi R}\left(\ln\frac{8R}{a}-\frac{1}{4}\right). \tag{21}$$

This comparison defines the cut-off parameter as $2\delta = \mathrm{e}^{1/4}$. The energy of two antiparallel uniform core vortices is

$$\mathcal{E} \sim \frac{\rho_\infty\kappa^2}{2\pi}\left[\ln\frac{h}{a}+\frac{1}{4}\right] \tag{22}$$

which, when written using the cut-off parameter, becomes

$$\mathcal{E} \sim \frac{\rho_\infty\kappa^2}{2\pi}\left[\ln\frac{h}{2a\delta}+\frac{1}{2}\right]. \tag{23}$$

The momentum and velocity of the vortex pair are given by (13). When the right-hand side of the expression (11) is evaluated using expressions (13) and (23) the result becomes

$$-\frac{\mathcal{E}}{\partial\mathcal{P}/\partial U}k^2 = \left(\frac{\kappa}{2\pi h}\right)^2 k^2\left[\ln\frac{h}{2a\delta}+\frac{1}{2}\right] \tag{24}$$

which differs from (18) by $\frac{1}{2}$. The nature of this difference together with a brief description of the cut-off method are given in the appendix.

The linear stability problem (7)–(9) was solved numerically for various h. The region of instability and the maximum growth rate were determined in the kh-plane (see figure 1). The stability boundary for the classical hollow core vortices is depicted in figure 1 as well.

3. Nonlinear evolution of the instability

As the unstable perturbation grows in amplitude, it can no longer be described by linear equations such as (7)–(9). To determine its subsequent evolution it is necessary to undertake

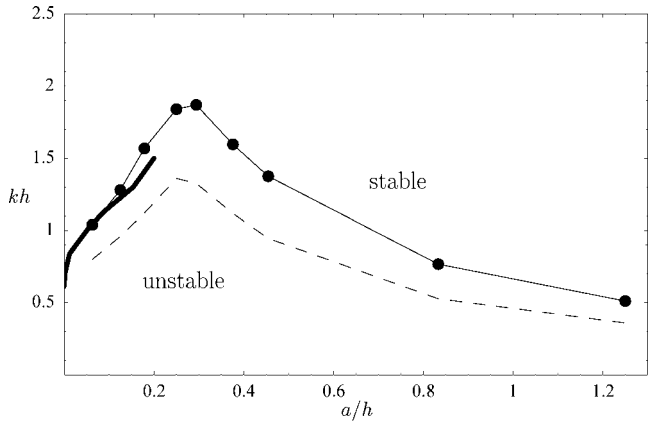

Figure 1. Stability boundary (dots and solid lines—for superfluid solitary waves, bold solid line—for classical hollow-core vortices) and maximum growth rate (dashed line) for (7)–(9).

direct numerical integrations of the GP equation. One can then understand the evolution in the following way. As the instability grows, it brings some segments of one line into closer proximity with corresponding segments of the other line, until the minimum distance between the lines reaches a critical value, approximately equal to the critical value ($h = h_c$) at which vorticity is lost on the solitary wave sequence (see section 2). At this moment, the Kelvin–Helmholtz theorem is inapplicable and reconnection occurs; curves of zero ψ on one line join with the curves of zero ψ on the other to form closed elongated vortex rings that later relax to become approximately circular. Before doing so, each ring oscillates in its fundamental mode, being alternatively prolate and oblate; the amplitude of this oscillation diminishes as it radiates acoustic waves.

This scenario is supported by direct numerical simulations, performed with the same numerical method as in our previous work [1]. In these computations we follow the evolution of a vortex pair moving in the x-direction in a computational box of dimensions $D_x = 60$, $D_y = 60$, $D_z = 120$. The xy-faces of the box are open to allow sound waves to escape; this is achieved numerically by applying the Raymond–Kuo technique [15]. The faces $z = 0$ and $z = D_z$ are reflective. To introduce an initial perturbation that does not favour any particular wavelength we start with the initial condition

$$\psi(x, y, z, t = 0) = \psi_0(x, y - 3) * \psi_0(x, y + 3) \tag{25}$$

where

$$\psi_0(x, y) = [1 - \exp(-0.7r^{1.15})] \exp(\mathrm{i}\theta) \tag{26}$$

is an approximation for the rectilinear vortex and r and θ are polar coordinates, such that $x = r\cos\theta$ and $y = r\sin\theta$. The wavelength of the instability for $h = 6$ was about 30, corresponding to $k \approx 0.2$, in good agreement with the result of the linear stability analysis, which gave $k \approx 0.19$. This wavelength determines where the vortex filaments approach each other and reconnect as vortex rings (see figure 2).

The reconnections are accompanied by the emission of sound waves and rarefaction pulses, resulting in line loss that is approximately one fourth of the total vortex line length, thus confirming that acoustic losses are significant and should be taken into account when modelling superfluid turbulence.

The results of our computations for other h are summarized in table 1 which gives energy, momentum and wavelength ℓ of the perturbation for the initial field and energy, momentum,

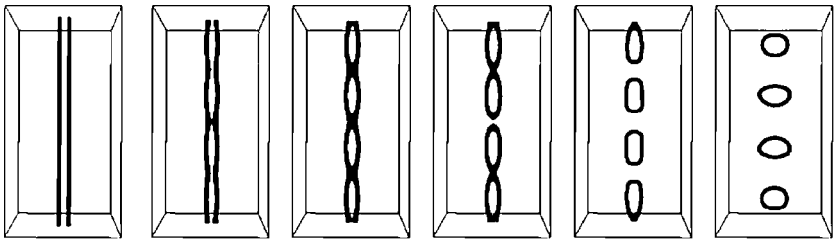

Figure 2. The isosurface $\rho/\rho_\infty = 0.2$ for two antiparallel vortices, initially distance $h = 6$ apart, which propel each other away from the viewer. An instability develops along the axes of these vortex lines and the lines reconnect to form circular vortex rings.

Table 1.

h	ℓ	$\mathcal{E}_{\rm init}$	$\mathcal{P}_{\rm init}$	$\mathcal{E}_{\rm ring}$	$\mathcal{P}_{\rm ring}$	$R_{\rm ring}$	% of line lost
8	53	819	2664	663	2612	11.5	32
6	33	450	1244	393	1204	7.8	26
3.6	16	167	362	125	228	3.3	35
2.2	14.6	107	201	–	–	–	100

and radius of the resulting vortex ring and the amount of vortex line lost as a percentage of the initial vortex line length. To reduce the time taken by an initial perturbation to grow, we took the initial ψ to be $\psi_0(x, y_+ + h/2) * \psi_0(x, y_- - h/2)$ where ψ_0 is given by (26), $y_\pm = y \pm 0.1 \cos kz$ and ψ_0 and k is the wavenumber for which the growth rate is a maximum according to the linear theory of section 2. Note that if h is small (though larger than the critical distance for the 2D vortex pair) the vortices annihilate each other and the energy is carried away as sound waves with the intermediate formation of 3D rarefaction pulses.

The increase in the percentage of line lost with h seen in the first two entries of table 1 may be explained by the following heuristic argument. If segments of length ℓ from the vortex pair are used to create a ring of radius R, the momentum $\rho\kappa\pi\ell$ of the segments must exceed the momentum $\rho\kappa\pi R^2$ of the ring, the difference being the momentum of the acoustic waves radiated during the reconnection process. Taking $\ell = 2\pi/k$ where k is the wavenumber of the fastest growing Crow instability for given h, we see therefore that

$$2h/k \geqslant R^2. \tag{27}$$

The line loss by the vortex pair is $2\ell = 4\pi/k$ of which $2\pi R$ is recovered by the ring. The fractional line loss is therefore $1-Rk/2$, and is smallest when equality holds in (27). Therefore

$$\text{minimum fractional line loss} = 1 - \sqrt{kh/2}. \tag{28}$$

This simple formula for k found by maximizing (19) gives 35% for $h = 8$, which is in good agreement with the 32% given in table 1. The minimum fractional line loss increases with h if $ka \ll 1$.

4. Conclusions

We studied the Crow instability for two antiparallel vortex lines obeying the GP equation. Linear stability analysis was used to determine the maximum growth rate of the instability and the region of instability. Through numerical simulations of the GP equation, we showed that

as perturbations grow to finite amplitude the lines reconnect to produce a sequence of almost circular vortex rings. We evaluated the resulting line loss.

Acknowledgments

We are grateful to Dr Sergey Nazarenko for useful discussions. This study is supported by the NSF grants DMS-9803480 and DMS-0104288.

Appendix. Classical Crow instability

Crow used the cut-off method to determine the growth rate, σ, of the instability in an incompressible fluid, for all kh and for $ka \ll 1$, where a is the radius of the vortex core [2]. This approximate method is based on the Biot–Savart law determining the fluid velocity, $\boldsymbol{v}(\boldsymbol{x})$, in an incompressible fluid from an assigned vorticity $\omega(\boldsymbol{x})$:

$$\boldsymbol{v}(\boldsymbol{x}) = \frac{1}{4\pi}\int \frac{\omega(\boldsymbol{x}')\times(\boldsymbol{x}-\boldsymbol{x}')}{|\boldsymbol{x}-\boldsymbol{x}'|^3}\,\mathrm{d}\boldsymbol{x}'. \tag{29}$$

It is supposed that the vorticity is confined to filaments of infinitesimal cross section so that (29) reduces to a line integral

$$\boldsymbol{v}(\boldsymbol{x}) = \frac{\kappa}{4\pi}\int \frac{\mathrm{d}\boldsymbol{s}'\times(\boldsymbol{x}-\boldsymbol{x}(s'))}{|\boldsymbol{x}-\boldsymbol{x}(s')|^3} \tag{30}$$

where s is the arc length on a filament and κ is the vorticity contained within it.

To determine the velocity, $\boldsymbol{U}(\boldsymbol{x})$, of the filament it is necessary to evaluate (30) for each point on the filament $\boldsymbol{x}(s)$, but the resulting integral (30) diverges. In the cut-off method the offending segment $|\boldsymbol{s}-\boldsymbol{s}'| < a\delta$ of the integral is arbitrarily removed, where δ is the cut-off parameter, the value of which depends on the core structure. This step is denoted by $[\delta]$:

$$\boldsymbol{U}(s) = \frac{\kappa}{4\pi}\int_{[\delta]} \frac{\mathrm{d}\boldsymbol{s}'\times(\boldsymbol{x}(s)-\boldsymbol{x}(s'))}{|\boldsymbol{x}(s)-\boldsymbol{x}(s')|^3}. \tag{31}$$

We give two examples. First, for our vortex pair, no divergence arises because $\mathrm{d}\boldsymbol{s}'$ and $\boldsymbol{x}(s)-\boldsymbol{x}(s')$ are parallel when s' and s are on the same line. Thus

$$U = \frac{\kappa h}{4\pi}\int_{-\infty}^{\infty}\frac{\mathrm{d}s}{(h^2+s^2)^{3/2}} = \frac{\kappa}{2\pi h}. \tag{32}$$

In the second case, a vortex ring of radius R ($\gg$a), (31) gives (14).

An alternative way of defining a cut-off is through the expression for the energy of a vortex line assembly. This is most conveniently expressed as in section 153 of [11] as

$$E = \frac{\rho}{8\pi}\int\int \frac{\omega(\boldsymbol{x})\cdot\omega(\boldsymbol{x}')}{|\boldsymbol{x}-\boldsymbol{x}'|}\,\mathrm{d}\boldsymbol{x}\,\mathrm{d}\boldsymbol{x}' \tag{33}$$

which, when the vorticity is concentrated into filaments is

$$E = \frac{\rho\kappa\kappa'}{8\pi}\int_{[\bar\delta]}\int_{[\bar\delta]} \frac{\mathrm{d}\boldsymbol{x}\cdot\mathrm{d}\boldsymbol{s}'}{|\boldsymbol{x}(s)-\boldsymbol{x}(s')|}\,\mathrm{d}\boldsymbol{x}\,\mathrm{d}\boldsymbol{x}' \tag{34}$$

and $[\bar\delta]$ signifies that the segment $|s'-s| < a\bar\delta$ is removed. Returning to our two examples, (34) gives

$$\mathcal{E} = \frac{\rho\kappa^2}{2\pi}\ln\frac{h}{2a\bar\delta} \tag{35}$$

for the vortex pair and

$$E = \frac{1}{2}\rho\kappa^2 R\left(\ln\frac{4R}{a\bar{\delta}} - 2\right) \tag{36}$$

for the thin-cored ring.

The cut-offs δ and $\bar{\delta}$ must be chosen differently. In order that the Hamiltonian relation

$$U = \partial E/\partial P \tag{37}$$

is obeyed by the ring, where $P = \rho\kappa\pi R^2$ is its momentum (impulse), it is necessary to hold the volume $2\pi^2 Ra^2$ of the ring constant in the differentiation (37) [16, 17]. This requirement, which implies that

$$\ln(\delta/\bar{\delta}) = \tfrac{1}{2} \tag{38}$$

is relevant even for the hollow core vortex, since any change in volume would imply that $p\,dV$ work is done on the system at infinity, with a concomitant change in E that would cause (37) to fail. Relations (35), (36) and (38) show that

$$\mathcal{E} = \frac{\rho\kappa^2}{2\pi}\left(\ln\frac{h}{2a\bar{\delta}} + \frac{1}{2}\right) \tag{39}$$

$$E = \frac{1}{2}\rho\kappa^2 R\left(\ln\frac{4R}{a\bar{\delta}} - \frac{3}{2}\right). \tag{40}$$

Result (40) agrees with known facts for the uniform-core $\left(\ln 2\delta = \frac{1}{4}\right)$ and hollow-core $\left(\ln 2\delta = \frac{1}{2}\right)$ rings [11, 19]. (The uniform-core vortex is one in which ω/ϖ is constant where $\omega\mathbf{1}_\phi$ is the vorticity and $\mathbf{1}_\phi$ is the unit vector in the direction of increasing ϕ and (ϖ, ϕ, z) are cylindrical coordinates; see section 165 of [11].) Similarly, for the vortex pair, $U = \partial\mathcal{E}/\partial\mathcal{P}$, where

$$\mathcal{P} = \rho\kappa h \tag{41}$$

is the momentum per unit length.

The expressions of Crow for the growth rates of his antisymmetric and symmetric modes of instability reduce, in the limit $kh \to 0$, to (10) and (11) above, but **not** with the expression (39) for $\mathcal{E}$. In its place stands

$$\hat{\mathcal{E}} = \frac{\rho\kappa^2}{2\pi}\left(\ln\frac{h}{2a\bar{\delta}} + 1\right). \tag{42}$$

It seems to us that this puzzling difference may be connected to the different frame of reference used in deriving (42). Crow used the co-moving frame, in which (42) translates to the energy $\tilde{\mathcal{E}} = \hat{\mathcal{E}} - \mathcal{P}U$:

$$\tilde{\mathcal{E}} = \frac{\rho\kappa^2}{2\pi}\ln\frac{h}{2a\bar{\delta}}. \tag{43}$$

For the reason why this does not coincide with (39) we offer the following speculation.

In the laboratory frame (the frame in which the fluid is at rest at infinity) the streamfunction $\psi(x, y)$ for a hollow core vortex pair is

$$\psi = \frac{\kappa}{2\pi}\ln\frac{r_2}{r_1} \tag{44}$$

where $r_1(r_2)$ is a distance from $\left(0, \frac{1}{2}h\right)$ $\left(\text{from } \left(0, -\frac{1}{2}h\right)\right)$; since these distances change with time, ψ is implicitly a function of t. The streaklines, i.e. the curves parallel to the instantaneous direction of the velocity $v = \nabla\times(\psi\mathbf{1}_z)$ are coaxial circles surrounding the cores, the surfaces

of which are (for $a \ll h$) $r_1 = a$ and $r_2 = a$. The energy per unit length is (see section 157 of [11])

$$\mathcal{E} = \tfrac{1}{2}\rho \int v^2 \, \mathrm{d}^3x = \tfrac{1}{2}\rho\kappa(\psi_{s1} - \psi_{s2}) = \rho\kappa\psi_{s1} \tag{45}$$

where $\psi_{s1}(\psi_{s2})$ is the value of ψ on the core surface, $r_1 = a$ ($r_2 = a$). This correctly reduces to (39) for $\ln 2\delta = \frac{1}{2}$.

Consider now the flow as seen in the co-moving frame. This consists of two parts: an interior region composed of (non-circular) streamlines surrounding the vortices and an exterior region where the steamlines start and finish at ∞, where $\boldsymbol{v} = -U\mathbf{1}_x$. The two regions are separated by an oblate dividing streamline, $x = \pm\left[\tanh(y/h) - y^2 - \frac{1}{4}h^2\right]^{1/2}$, on which $\tilde{\psi} = 0$ (see the figure on p 221 of [11]). Here

$$\tilde{\psi} = -Uy + \psi = -\frac{\kappa}{2\pi}\left(\frac{y}{h} + \ln\frac{r_1}{r_2}\right) \tag{46}$$

is the streamfunction in the co-moving frame.

Since the interior fluid is, as seen in the laboratory frame, perpetually carried along by the vortex in its motion, it has a special significance. Its energy is (cf (45))

$$\rho\kappa\tilde{\psi}_{s1} = \frac{\rho\kappa^2}{2\pi}\left(\ln\frac{h}{a} - \frac{1}{2}\right) = \frac{\rho\kappa^2}{2\pi}\ln\frac{h}{2a\delta} = \tilde{\mathcal{E}}. \tag{47}$$

The same argument applies with minor modifications to vortices with other internal structure.

References

[1] Berloff N G and Roberts P H 2000 *J. Phys. A: Math. Gen.* **33** 4025
[2] Crow S C 1970 *AIAA* **8** 2172
[3] Donnelly R J 1991 *Quantized Vortices in Helium II* (Cambridge: Cambridge University Press)
[4] Fetter A L and Svidzinsky A A 2001 *J. Phys.: Condens. Matter* **13** R135
[5] Ford R and Llewellyn Smith S G 1999 *J. Fluid. Mech.* **386** 305
[6] Jones C A and Roberts P H 1982 *J. Phys. A: Math. Gen.* **15** 2599
[7] Jones C A, Putterman S J and Roberts P H 1986 *J. Phys. A: Math. Gen.* **19** 2991
[8] Koplik J and Levine H 1993 *Phys. Rev. Lett.* **71** 1375
[9] Koplik J and Levine H 1996 *Phys. Rev. Lett.* **76** 4745
[10] Kuznetsov E A and Rasmussen J 1995 *Phys. Rev.* E **51** 4479
[11] Lamb H 1945 *Hydrodynamics* 6th edn (New York: Dover)
[12] Leadbeater M, Winiecki T, Samuels D C, Barenghi C F and Adams C S 2001 *Phys. Rev. Lett.* **86** 1410
[13] Moore D W 1972 *Aero. Quart.* **23** 307
[14] Pitaevskii L P 1961 *Sov. Phys.–JETP* **13** 451
[15] Raymond G W and Kuo H L 1984 *Q. J. R. Meteorol. Soc.* **110** 525
[16] Roberts P H and Donnelly R J 1970 *Phys. Lett.* A **31** 137
[17] Roberts P H 1972 *Mathematica* **19** 169
[18] Roberts P H and Grant J 1971 *J. Phys. A: Math. Gen.* **4** 55
[19] Saffman P G 1992 *Vortex Dynamics* (Cambridge: Cambridge University Press)
[20] Schwarz K W 1988 *Phys. Rev.* B **38** 2398
[21] Vinen W F 2000 *Phys. Rev.* B **61** 1410